Available online at www.sciencedirect.com
SCIENCE DIRECT®
Journal of Catalysis 223 (2004) 250–261
JOURNAL OF CATALYSIS
www.elsevier.com/locate/jcat

Photocatalytic oxidation of methyl formate on TiO_2: a transient DRIFTS study

Adrienne C. Lukaski and Darrin S. Muggli *

Department of Chemical Engineering, University of North Dakota, Grand Forks, ND 58202-7107, USA

Received 23 July 2003; revised 22 December 2003; accepted 22 December 2003

Abstract

Methyl formate adsorbs both molecularly and dissociatively as methoxy and formate on titanium dioxide (TiO_2). Methyl formate dissociates on TiO_2 at dual sites that adsorb methoxy and formate; formate adsorption sites are more numerous than those of methoxy and the availability of methoxy sites limits methyl formate coverage. Photocatalytic oxidation (PCO) oxidizes the α-carbon in methyl formate to CO_2 without forming any long-lived intermediates, whereas the β-carbon forms CO_2 through formaldehyde and formate. At least two types of active sites exist for PCO on TiO_2 and their activities differ by more than an order of magnitude; the more-active sites comprise approximately 30% of adsorption sites. Photocatalytic oxidation carried out at 373 K oxidizes species more quickly than at room temperature because elevated temperatures enhance inherent site activity and convert adsorbed methoxy to formate. Water does not poison methyl formate PCO and redistributes weakly bound species during PCO by displacement. Water preferentially displaces methanol and also converts some adsorbed methoxy to formate at room temperature.

Keywords: Methyl formate; Methoxy; Formate; Photocatalytic oxidation; TiO_2; Transient reaction; DRIFTS

1. Introduction

Heterogeneous photocatalytic oxidation (PCO) has potential applications for the treatment of waste streams with dilute concentrations of VOCs because it oxidizes a wide range of both liquid- and vapor-phase organics to environmentally benign compounds at room temperature [1–12]. Photocatalytic oxidation employs UV or near-UV irradiation to oxidize adsorbed organics to CO_2 and H_2O on semiconductor catalysts, such as titanium dioxide (TiO_2). Previous studies have demonstrated that PCO successfully oxidizes many gas-phase organics, but reaction pathways are not fully understood and intermediates are often not identified [1–4,7,9,11,12].

Popova et al. [13] identified bidentate formate and two forms of molecularly adsorbed MF, H bonded and coordinatively bonded, on TiO_2 after MF adsorption at 373 K by in situ FTIR spectroscopy. Similarly, Liao et al. [14] reported that formic acid adsorbed on TiO_2 molecularly and dissociatively as formate with bridging coordination. Chuang et al. [15] reported that methanol also adsorbed molecularly and dissociatively as methoxy on TiO_2. Busca et al. [16] found that methoxy adsorbed covalently with surface VOH groups in a monodentate configuration on vanadium-supported TiO_2. Because methyl formate (MF) adsorbs both molecularly and dissociatively as methoxy and formate, a study of MF adsorption and PCO is an important step in characterizing surface reactions on TiO_2 and follows naturally as a progression of previous studies [13–15,17–22].

Chuang et al. [18], in a novel study of MF PCO, examined thermal reaction and photochemistry of MF on TiO_2. Using FTIR spectroscopy, the authors reported that MF adsorbed molecularly and dissociatively as methoxy and formate species on TiO_2 at 308 K. During MF PCO, they observed an immediate decrease of MF absorptions with concomitant formation of CH_2O, CO, CO_2, and H_2O in the gas phase. The authors attributed the evolution of CO and CO_2 to adsorbed formate, whereas methoxy formed CH_2O, in agreement with previous studies [20–25]. Upon heating the catalyst to 423 K, Chuang et al. [18] observed near-complete disappearance of molecularly adsorbed MF and concluded that the surface consisted primarily of formate, methoxy, and an orthoester-type intermediate.

* Corresponding author.
E-mail address: darrin_muggli@und.nodak.edu (D.S. Muggli).

0021-9517/$ – see front matter
doi:10.1016/j.jcat.2003.12.015

Although MF formation and adsorption have been widely researched, no study has attempted to characterize MF adsorption sites on TiO_2 or to extensively examine the reaction pathways of MF PCO; only one study investigated the photochemistry of MF on TiO_2 [18]. Although previous work by Chuang et al. [18] provided information about MF adsorption and reaction on TiO_2, surface species may not be fully characterized under steady-state conditions because the presence of gas-phase species complicates interpretation of infrared spectra. In contrast, transient PCO takes place in the absence of gaseous organics and separates adsorption, surface reaction, and desorption steps in time.

In this study, transient reaction techniques and temperature-programmed oxidation (TPO) were combined with FTIR spectroscopy to investigate the reaction pathway of MF on TiO_2. The implementation of isotope labels in ^{13}MF ($H\,^{13}COOCH_3$) and deuterated MF (D-MF, $DCOOCH_3$) is a unique aspect of this study that provides justification for spectral band assignments and information about MF adsorption and PCO. In addition to identifying adsorbed species, this study explores the effects of H_2O and heating on surface species. This study also quantifies the surface concentrations and relative activities of multiple active sites for MF PCO on TiO_2 and determines that the availability of methoxy adsorption sites limits MF coverage.

2. Experimental methods

2.1. Transient photocatalytic oxidation with mass spectrometry

The experimental apparatus used in this study has been described previously [7,10,11,26]. Using the same apparatus and procedure as this study, previous work [7–11,17,27–32] investigated the uniformity of UV irradiation, surface and gas-phase diffusion limitations, temperature gradients, and other possible experimental artifacts and found them to be insignificant. An annular Pyrex reactor allowed for high gas-flow rates and uniform UV irradiation of the catalyst. A thin layer of approximately 30 mg of Degussa P-25 TiO_2 coated the inner surfaces of the photoreactor (with a 1-mm annular gap). A furnace, which consisted of Ni–Cr wire wrapped around a quartz cylinder, encased the reactor and six 8-W UV lamps (Johnlite) surrounded the furnace. A 0.5-mm chromel-alumel, shielded thermocouple contacted the catalyst film to provide feedback to the temperature controller. A Balzers QMS 200 quadrupole mass spectrometer monitored the reactor effluent directly downstream of the reactor.

Before each isothermal PCO, the catalyst was heated at a rate of 1 K/s to 723 K in 100 sccm flow of 20% O_2 in He (Praxair, UHP) and held at this temperature for 20 min to create a reproducible surface. Two pulses of MF (420 μmol/g catalyst each) injected upstream of the reactor saturated the catalyst and the carrier gas flushed excess organic from the gas phase. Before transient PCO, a shield blocked UV light from the reactor for 10 min as the lights reached a steady output. Removing the shields exposed the catalyst to UV irradiation and, thus, initiated transient PCO. After 20 min, terminating UV irradiation stopped PCO and subsequent TPO oxidized remaining surface species. Temperature-programmed oxidation was performed in the same carrier gas flow as PCO by heating the catalyst (1 K/s) to 723 K and holding at this temperature until products were no longer detected in the gas phase.

2.2. Transient photocatalytic oxidation with DRIFTS

The infrared study utilized a FTIR spectrophotometer (Thermo Nicolet 670) equipped with a MCT-A detector that was cooled with liquid nitrogen. The reaction system consisted of a praying mantis diffuse reflectance FTIR spectroscopy (DRIFTS) accessory (Harrick Scientific, DRP) that was modified with a reaction cell (Harrick Scientific, HVC-DRP) to facilitate gas flow through the system. The reaction cell was equipped with a heater and housed a sample cup filled with TiO_2. A dome with three windows covered the sample cup and was held in place with retaining plates; two of the windows were IR transparent (KBr), while the third allowed for UV irradiation of the catalyst (quartz). A mass-flow controller (Tylan FC-260) maintained 100 sccm of 20% O_2 in He (Praxair UHP), while a purge gas generator (Parker Balston 7545 NA) provided air for system purge.

The catalyst was heated at a rate of 1 K/s to 723 K in 20% O_2 flow and held at this temperature for 20 min to provide a clean surface. Omnic software (Thermo Nicolet Corporation) recorded interferograms over the interval of 650–4000 cm^{-1} by averaging 64 scans with a resolution of 4 cm^{-1}. After cooling to room temperature, a background spectrum of the clean TiO_2 surface was collected. Subtraction of the background spectrum from subsequent sample spectra distinguished bands of surface compounds by removing TiO_2 absorptions. After background collection, three pulses of MF (420 μmol/g catalyst each) saturated the catalyst surface and the carrier gas flushed excess organic from the gas phase for 90 min prior to PCO; spectra collected during organic adsorption tracked the removal of gas-phase species from the system. A 350-W Hg arc lamp (Exfo Corp) equipped with a 320- to 390-nm filter and a liquid-filled light guide (5 mm × 1000 mm) provided UV irradiation for PCO experiments. A radiometer (Exfo) determined the power emitted from the tip of the light guide to be ~ 1.55 W/cm^2; a distance of approximately 2 cm separated the light guide from the catalyst. Collecting spectra after various irradiation times monitored the progression of PCO and provided qualitative information about the surface reaction. Previous band assignments and characteristic regions of functional groups [13–15,19,33,34], in conjunction with isotope shifts, identified absorption bands of surface species.

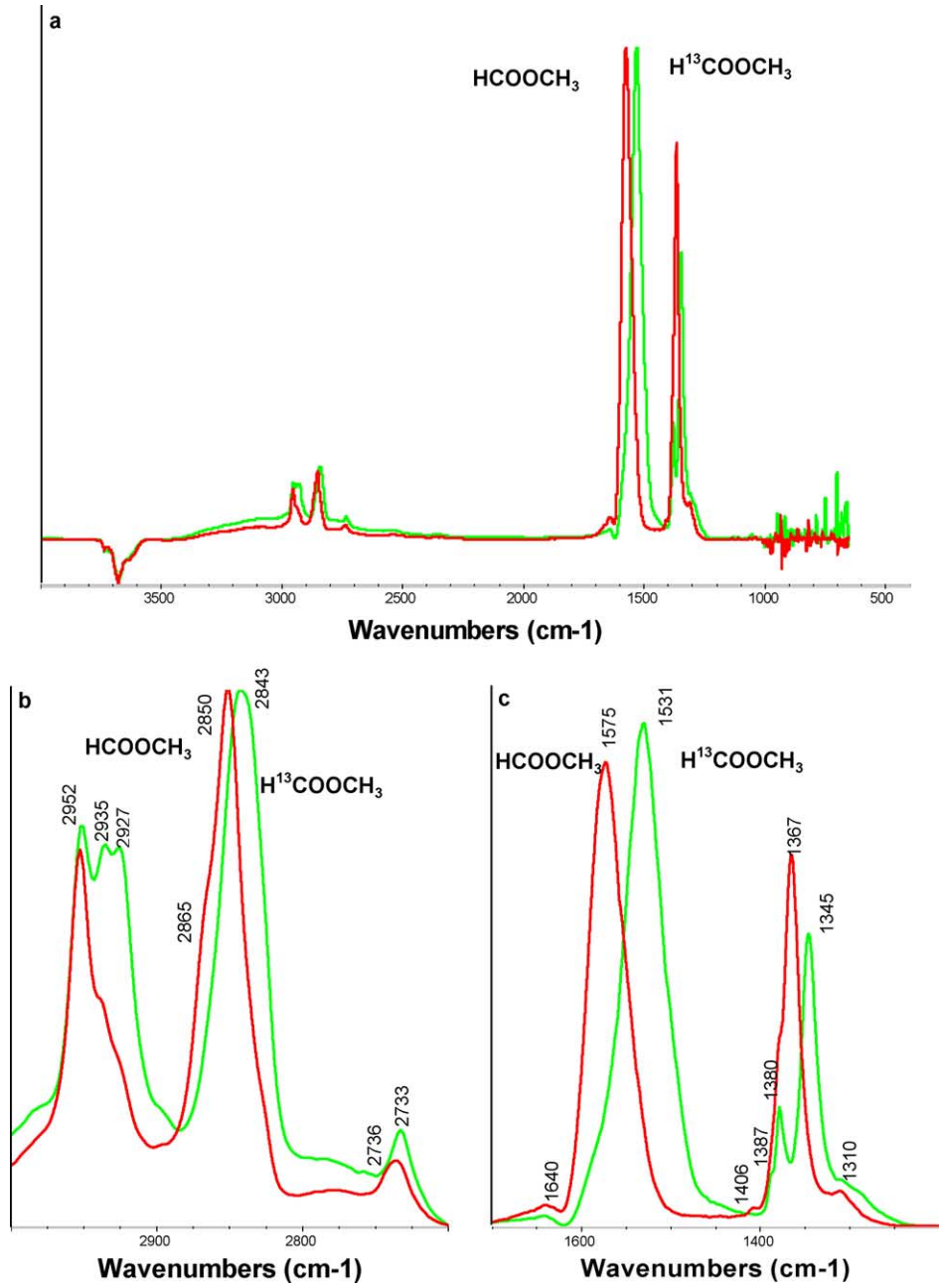

Fig. 1. Infrared spectra (a) of $HCOOCH_3$ and $H^{13}COOCH_3$ adsorbed at room temperature on fresh TiO_2 with vibrational modes in the alkyl (b) and carboxylate (c) regions.

3. Results

3.1. Methyl formate adsorption

Fig. 1 shows DRIFTS spectra of ^{12}MF and ^{13}MF ($H^{13}COOCH_3$) adsorbed on TiO_2 at room temperature; the y axis, which is not shown for clarity, is expressed in Kubelka-Munk units on a common scale. The isotope label in ^{13}MF red-shifted the frequencies of vibrational modes associated with the α-carbon in MF. Table 1 summarizes the absorption spectra of ^{12}MF and ^{13}MF. In agreement with previous studies [13,18], Fig. 1 shows that methyl formate adsorbs on TiO_2 both molecularly and dissociatively as methoxy and formate.

Wu et al. [35] attributed signals at 2948 and 2926 cm^{-1} to surface methanol and methoxy adsorbed on TiO_2, respectively, while Chuang et al. [18] observed bands at 2960, 2938, and 2928 cm^{-1} following MF adsorption on TiO_2. Infrared spectra of methanol adsorbed at room temperature on TiO_2 (not shown) exhibited absorptions at 2949, 2924, 2845, and 2821 cm^{-1}. In this study, the term methoxy will refer to dissociative adsorption of the β-carbon in MF whether it adsorbs as CH_3O or interacts with surface hydroxyls to form adsorbed methanol.

Table 1
Comparison of vibrational frequencies (cm^{-1}) of $HCOOCH_3$ and $H\,^{13}COOCH_3$ adsorbed on TiO_2 at room temperature

$HCOOCH_3$	$H\,^{13}COOCH_3$	Red shift	Band assignment
2952	2952	0	Methoxy
2935	2935	0	Methyl formate
2927	2927	0	Methyl formate
2865	2843	22	Formate
2850		NA	Methoxy
2736	2733	3	Methyl formate
1640	1640	0	β-Carbon formate
1575	1531	44	α-Carbon formate
1406	1387	19	α-Carbon formate
1380	1380	0	β-Carbon formate
1367	1345	22	α-Carbon formate
1310	1310	0	Methyl formate

Alkyl CH_x stretching in surface methoxy characterizes the absorption at 2952 cm^{-1} because the isotope label in ^{13}MF did not red-shift this band (Fig. 1b). Additionally, DRIFTS spectra of D-MF (not shown) exhibited a signal of intensity similar to those in Fig. 1b at this wavenumber. Because methoxy originates from dissociative adsorption of the β-carbon in MF (always carbon-12 in this study), carbon-13 ($H\,^{13}COOCH_3$) and deuterium ($DCOOCH_3$) isotopic substitutions on the α-carbon in MF would not affect methoxy absorptions.

Carbon-13 typically red-shifts C–H stretching frequencies by ~ 10 cm^{-1} [34] and is expected to affect absorption *intensities* of vibrational modes, even for those atoms not bonded directly to the isotope. Infrared spectra of other molecules [36] showed that carbon-13 labeling changed the intensity of several absorption bands that were not red shifted. Fig. 1b shows that the isotope label in ^{13}MF increased the intensity of bands at 2935 and 2927 cm^{-1}, yet did not red-shift these absorptions. Replacing hydrogen on the α-carbon in MF with deuterium (not shown) had a similar effect on the bands at 2935 and 2927 cm^{-1}. If these absorptions represented CH stretching modes of the α-carbon in MF, the isotope labels would red-shift these signals and replacing α-hydrogen with deuterium would induce greater shifts than the carbon-13 label. However, deuterium and carbon-13 would have a similar effect on vibrational modes of the β-carbon in MF because the mass of the carboxylate group (DCOO and $H\,^{13}COO$) in both isotopic species is the same. Therefore, absorptions at 2935 and 2927 cm^{-1} were assigned to CH stretching of the methyl group (β-carbon) in molecularly adsorbed MF.

Because the isotope label in ^{13}MF formed one band (2843 cm^{-1}) from two ^{12}MF absorptions (2865 and 2850 cm^{-1}) (Fig. 1b), vibrational modes associated with both carbons in MF evidently overlap in this region. Carbon-13 apparently red-shifted the signal at 2865 cm^{-1}, which, in turn, covered the band at 2850 cm^{-1}. Therefore, the absorption at 2865 cm^{-1} may characterize CH stretching in α-carbon formate or in molecularly adsorbed MF. Because DRIFTS spectra of formic acid isotopes ($H\,^{12}COOH$ and $H\,^{13}COOH$) (not shown) exhibited a similar red shift from 2870 to 2855 cm^{-1}, the absorption at 2865 cm^{-1} appears to characterize formate derived from the α-carbon in MF. The band at 2850 cm^{-1}, which did not appear to shift in Fig. 1b, was attributed to CH stretching in surface methoxy.

Chuang et al. [18] identified 1675 cm^{-1} as carbonyl stretching in formic acid on TiO_2 because heating to 423 K decreased this band and gas-phase formic acid absorbs near 1740 cm^{-1}, while Popova et al. [13] found that carbonyl stretching in formic acid coordinatively bonded to Lewis acid sites on TiO_2 characterized 1665 cm^{-1}. In this study, absorption at 1640 cm^{-1} was assigned to carbonyl stretching in formate species derived from the β-carbon in MF because carbon-13 typically red-shifts C=O stretching frequencies by ~ 40 cm^{-1} [34] and the isotope label in ^{13}MF (Fig. 1c) did not shift this band.

The isotope label on ^{13}MF red-shifted the bands at 1575 and 1367 cm^{-1} (Fig. 1c), and therefore these absorptions were assigned to asymmetric and symmetric COO^- stretching in α-carbon formate dissociated from MF, respectively, in agreement with previous work [14,33]. Additionally, DRIFTS spectra of HCOOH and $H\,^{13}COOH$ (not shown) showed that carbon-13 induced similar red shifts at 1563 and 1362 cm^{-1}.

The isotope label in ^{13}MF red-shifted the α-carbon formate band from 1406 to 1387 cm^{-1} (Fig. 1c); this absorption was assigned to α-carbon formate in agreement with Liao et al. [14]. The isotope label in ^{13}MF red-shifted the α-carbon formate band from 1367 to 1345 cm^{-1} and revealed a well-defined signal at 1380 cm^{-1} that appeared as a shoulder in the ^{12}MF spectrum (Fig. 1c). Because both ^{12}MF and ^{13}MF exhibited absorptions at 1380 cm^{-1}, this signal was attributed to formate derived from the β-carbon in MF. Infrared spectra of D-MF and formic acid (not shown) exhibited comparable bands at 1380 cm^{-1}, while a weaker absorption appeared in methanol DRIFTS spectra (not shown). This indicates that formate produced from the interaction of adsorbed methoxy (β-carbon in MF) with lattice oxygen absorbs at this frequency. In agreement, 1380 cm^{-1} appears to characterize formate, which is a PCO intermediate of the β-carbon in MF, because DRIFTS spectra of ^{13}MF, D-MF, and methanol PCO showed that the intensity of this absorption increased initially upon UV irradiation and decreased at longer reaction times.

3.2. Transient PCO of methyl formate

Fig. 2a shows the gas-phase products during transient PCO of a ^{13}MF monolayer at room temperature on TiO_2. Upon UV irradiation of the catalyst at 60 s, the α-carbon in ^{13}MF oxidized quickly to $^{13}CO_2$. After reaching an initial maximum, the $^{13}CO_2$ decay curve in Fig. 2a exhibited three regions: during the initial 100 s of PCO, the $^{13}CO_2$ formation rate decreased slowly, then declined quickly over the next 400 s, and dropped more slowly than initially at longer reaction times. As shown previously [17], the for-

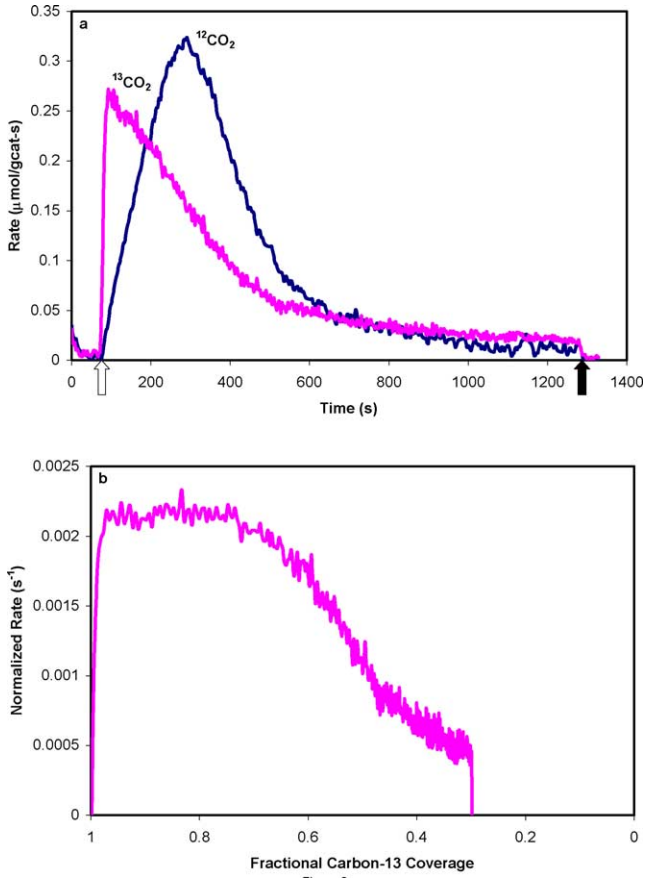

Fig. 2. Formation rates (a) and normalized $^{13}CO_2$ formation rate (b) during transient PCO of H$^{13}COOCH_3$ on TiO_2 at room temperature. The UV lights were turned on (arrow) at 60 s and turned off (arrow) at 1260 s.

mation of gas-phase CO_2 monitors the surface reaction rate because CO_2 does not adsorb significantly on TiO_2 at room temperature. That is, the evolution of gas-phase CO_2 is not desorption limited and measures the surface PCO rate directly.

The immediate maximum in the $^{13}CO_2$ formation rate (Fig. 2a) indicates that the α-carbon in MF oxidized directly to CO_2 without forming any long-lived intermediates. In contrast, the β-carbon formed CO_2 slowly and the maximum $^{12}CO_2$ formation rate occurred after approximately 230 s of UV irradiation (Fig. 2a). After 20 min of PCO, TPO oxidized the remaining surface species to ^{12}CO, ^{13}CO, and H_2O. The amounts of CO_2 that formed during transient PCO, combined with those of CO that desorbed during subsequent TPO, quantified ^{13}MF coverage. Repeat experiments determined ^{13}MF coverage to be 140 ± 10 μmol/g-catalyst (95% confidence limits). The total CO_2 rate in Fig. 2a, as well as ^{13}MF coverage, was the same as that during ^{12}MF PCO (not shown), which indicates that gas-phase species were identified correctly.

To explore the activities of adsorption sites, the $^{13}CO_2$ formation rate was normalized by dividing it by the amount of carbon-13 species that remained adsorbed at each sample point. For a single-step reaction, such as oxidation of the α-carbon in MF (discussed later), this analysis measures directly the activity of TiO_2 adsorption sites. For the β-carbon in MF, the formation of surface intermediates complicates the analysis of the normalized $^{12}CO_2$ formation rate and, therefore, it is not plotted. The normalized $^{13}CO_2$ formation rate (Fig. 2b) reached an initial maximum of 2.3×10^{-3} s^{-1} and decreased after approximately 30% of carbon-13 species reacted. Catalyst activity decreased more quickly than ^{13}MF coverage and the normalized $^{13}CO_2$ formation rate was approximately 20% of the initial value (5×10^{-4} s^{-1}) at low coverages. If all of the adsorption sites were equally active, the normalized rate would be constant for a first-order, single-step reaction. Although a second-order reaction could produce a normalized $^{13}CO_2$ formation rate similar to that in Fig. 2b, the rate normalized by the square of coverage (not shown) also decreased with time during PCO. Alternatively, Fig. 2b suggests more than one type of active site for PCO.

Fig. 3 shows DRIFTS spectra of surface species during ^{12}MF PCO at room temperature on TiO_2 (note that the UV intensity used in the DRIFTS study was much greater than that used during PCO experiments with mass spectrometric detection and, therefore, the time scales are not comparable). Upon UV irradiation, dissociatively adsorbed MF bands assigned to methoxy at 2952 and 2850 cm^{-1} (Fig. 3a) and formate at 1575, 1406, and 1367 cm^{-1} (Fig. 3b) decreased quickly. Formate absorptions at 1575, 1406, and 1367 cm^{-1} decreased more quickly than those at 1640, 1556, and 1380 cm^{-1}. In agreement with transient PCO (Fig. 2b), Fig. 3 suggests multiple active sites for MF PCO on TiO_2 because UV irradiation did not decrease absorption bands at the same rate.

Photocatalytic oxidation quickly decreased the molecularly adsorbed MF absorption at 2736 cm^{-1} and revealed an underlying band at 2743 cm^{-1} that decreased slowly in Fig. 3a. Because 2743 cm^{-1} appeared in DRIFTS spectra during ^{13}MF, D-MF, and methanol PCO (not shown), this absorption evidently characterizes an intermediate of methoxy PCO. This intermediate is most likely formate because infrared spectra of formic acid adsorbed on TiO_2 (not shown) showed a similar absorption at 2738 cm^{-1}. Furthermore, the appearance of strong absorptions in the carboxylate (1640 and 1380 cm^{-1}) and alkyl (2865 cm^{-1}) regions of DRIFTS spectra during methanol PCO clearly showed that methoxy oxidized to formate.

3.3. Transient PCO of methyl formate adsorbed at 373 K

Fig. 4a shows transient PCO in which ^{13}MF was adsorbed on TiO_2 at 373 K before the catalyst was cooled to perform room-temperature PCO. The results of another experiment, in which the catalyst was heated to 373 K after adsorbing a ^{13}MF monolayer and then cooled to room temperature for PCO, were identical to those in Fig. 4a. Preheating to 373 K reduced carbon-12 coverage by approximately 30%, yet did not change carbon-13 coverage. Upon UV irradiation, the $^{13}CO_2$ formation rate (Fig. 4a) quickly reached a maximum

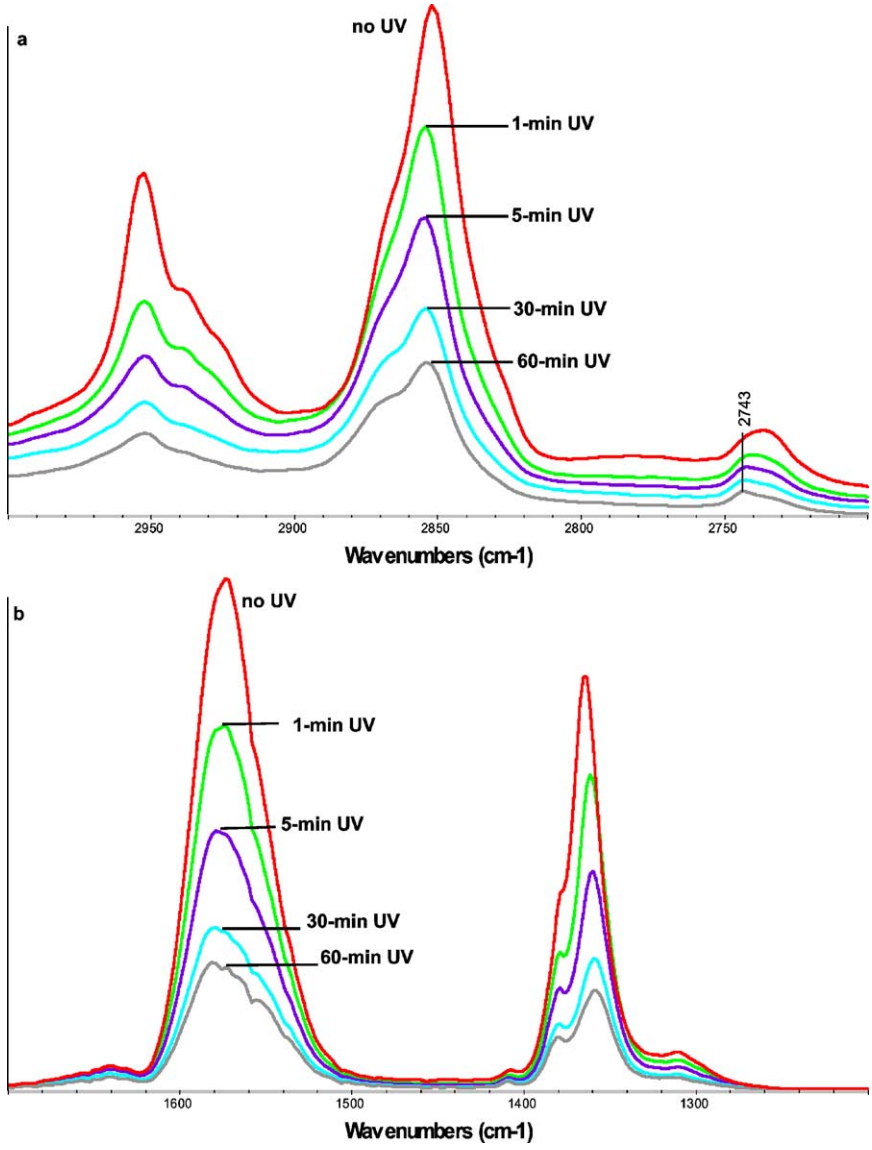

Fig. 3. Infrared spectra of $HCOOCH_3$ before PCO at room temperature on fresh TiO_2 and after various UV irradiation times with vibrational modes in the alkyl (a) and carboxylate (b) regions.

that was approximately 20% *greater* than that in Fig. 2a. The maximum $^{12}CO_2$ formation rate during PCO with preheating was approximately 75% of that during PCO with room-temperature adsorption, yet the maximum occurred approximately 130 s earlier (Fig. 5). After 100 s of UV irradiation, the $^{12}CO_2$ formation rate during PCO with preheating was approximately 1.3 times that without preheating (Fig. 5). The normalized $^{13}CO_2$ formation rate during PCO with preheating (Fig. 4b) quickly reached a maximum of 2.5×10^{-3} s^{-1} and began to decrease after approximately 15% of carbon-13 species reacted, whereas that in Fig. 2b began to decrease after 30% of the carbon-13 reacted.

Fig. 6 shows DRIFTS spectra of MF that was adsorbed on TiO_2 at 373 K before the catalyst was cooled to room temperature, as well as MF coadsorbed with H_2O (discussed later). Fig. 6 also shows DRIFTS spectra of a MF monolayer adsorbed at room temperature for comparison. Adsorption at 373 K decreased methoxy and molecularly adsorbed MF bands at 2952, 2935, 2927, 2850, 2736, and 1310 cm^{-1} (Fig. 6a). That is, preheating apparently reduced the carbon-12 coverage in Fig. 4 by removing methoxy species before PCO. Although the decreased bands at 2935, 2927, 2736, and 1310 cm^{-1} (Fig. 6) could be interpreted as MF removal, mass balances show that heating did not reduce carbon-13 coverage. Instead, molecularly adsorbed MF that was displaced by heating (2935, 2927, 2736, and 1310 cm^{-1}) appears to readsorb dissociatively on sites vacated by methoxy removal.

Preheating to 373 K increased the intensity of the β-band at 2743 cm^{-1} (Fig. 6a), which indicates that elevated temperatures converted some methoxy to formate (Fig. 3a). Additionally, the methoxy absorption at 2850 cm^{-1} slightly

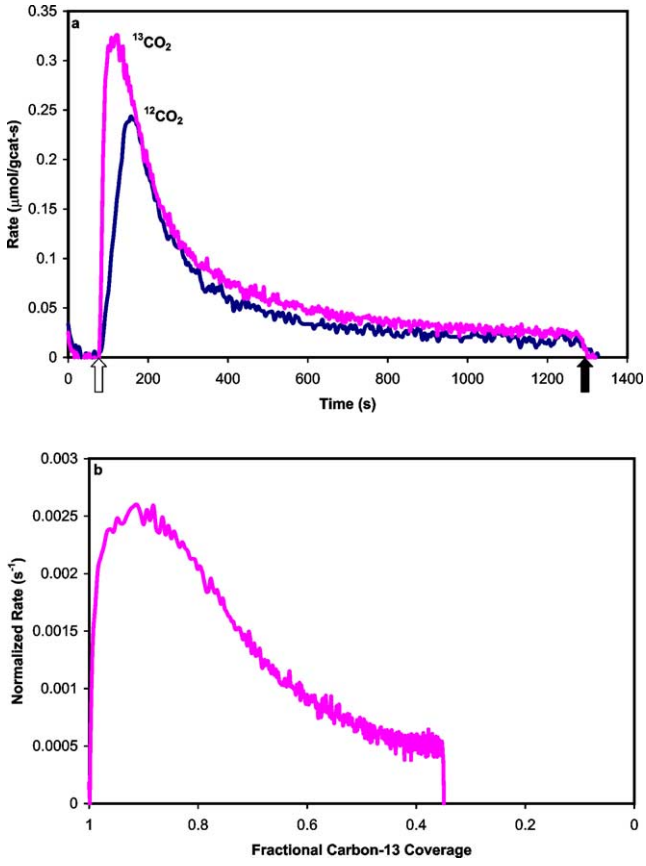

Fig. 4. Formation rates (a) and normalized $^{13}CO_2$ formation rate (b) during room-temperature transient PCO of H $^{13}COOCH_3$ on TiO_2 with preheating to 373 K. The UV lights were turned on (arrow) at 60 s and turned off (arrow) at 1260 s.

blue-shifted to 2853 cm^{-1} in Fig. 6b. Because formates derived from both carbons in MF (2865 cm^{-1}) and methoxy (2845 cm^{-1}) exhibit overlapping absorptions in this region, the blue-shifted methoxy band suggests that preheating increased the concentration of formate species relative to that of methoxy. That is, preheating evidently removed methoxy species and increased formate coverages by displacing MF, which readsorbed dissociatively on the sites vacated by methoxy removal.

Fig. 6b also shows that preheating shifted the α-carbon formate absorption band from 1367 to 1361 cm^{-1} and increased the intensity of this red-shifted signal (1361 cm^{-1}). This suggests that α-carbon formate coverage increased. Although Fig. 6b shows that preheating did not significantly increase the band at 1575 cm^{-1}, repeatedly adsorbing MF at room temperature and heating the catalyst to 373 K (not shown) also increased the intensity of this α-carbon formate absorption. Similar to Fig. 1c, the apparent decrease in the intensity of the β-carbon formate band at 1380 cm^{-1} is at least in part the result of the red shift from 1367 to 1361 cm^{-1} because absorptions characterizing formate derived from both carbons in MF overlap in this region.

To further explore the role of heating, ^{13}MF PCO was carried out at 373 K. Although room-temperature PCO with

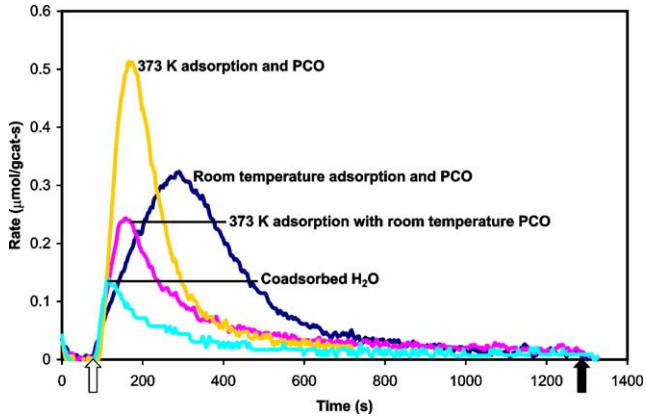

Fig. 5. $^{12}CO_2$ formation rates during transient PCO of H $^{13}COOCH_3$ at room temperature, with preheating to 373 K, and with coadsorbed H_2O. The UV lights were turned on (white arrow) at 60 s and turned off (black arrow) at 1260 s.

preheating (Fig. 4) and PCO at 373 K (Fig. 7) resulted in comparable carbon-13 and -12 coverages, the maximum $^{13}CO_2$ and $^{12}CO_2$ formation rates during PCO at 373 K (Fig. 7a) were approximately twice those seen in Fig. 4a. The initial catalyst activity during PCO at 373 K (Fig. 7b) was 2.7 times that during room-temperature PCO (Fig. 2b), yet the normalized $^{13}CO_2$ formation rate in Fig. 7b decreased after approximately 25% of carbon-13 species reacted.

3.4. Transient PCO of coadsorbed methyl formate and H_2O

Fig. 8 shows transient PCO of ^{13}MF with coadsorbed H_2O; 2 μL of H_2O was injected in the dark after adsorbing a ^{13}MF monolayer on TiO_2. Coadsorbing H_2O removed approximately 50% of carbon-12 species, yet did not change carbon-13 coverage. During PCO with coadsorbed H_2O (Fig. 8a), the α-carbon in MF initially oxidized to $^{13}CO_2$ at approximately twice the rate seen in Fig. 2a. In contrast, the maximum $^{12}CO_2$ formation rate was approximately 45% of that during room-temperature PCO (Fig. 5). However, the maximum $^{12}CO_2$ formation rate during PCO with coadsorbed H_2O occurred approximately 170 s earlier than that during PCO of a ^{13}MF monolayer (Fig. 5). After 60 s of PCO, the $^{12}CO_2$ formation rate during PCO with coadsorbed H_2O was approximately 1.3 times that during PCO of a monolayer (Fig. 5).

Fig. 6 shows DRIFTS spectra of MF coadsorbed with H_2O on TiO_2. Similar to preheating, coadsorbing H_2O removed methoxy and molecularly adsorbed MF (2952, 2935, 2927, 2850, 2736, and 1310 cm^{-1}) and increased α-carbon formate coverage (2865, 1575, and 1367 cm^{-1}) (Fig. 6). As previously discussed, this suggests that coadsorbing H_2O displaced weakly bound, molecularly adsorbed MF, which readsorbed dissociatively on sites vacated by methoxy removal. Additionally, coadsorbing H_2O converted some methoxy to formate (2743, 2865, and 1640 cm^{-1}).

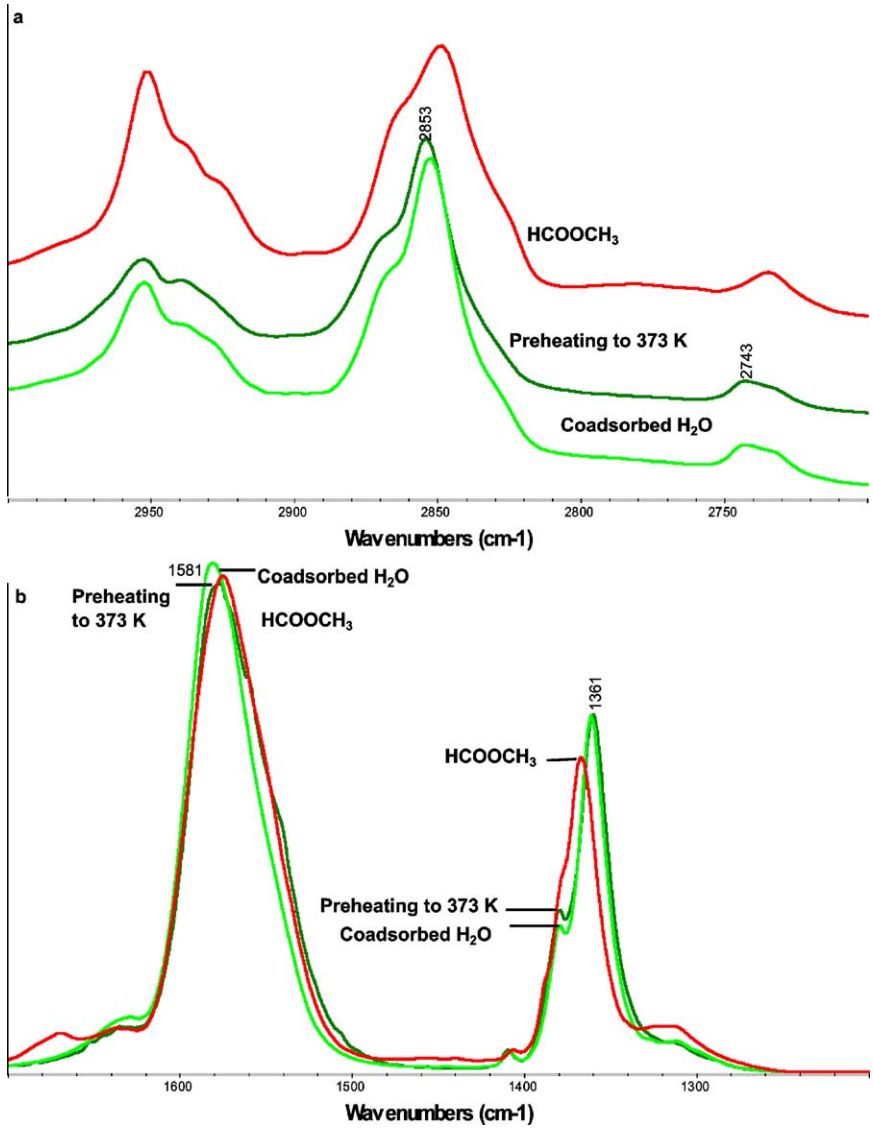

Fig. 6. Infrared spectra of $HCOOCH_3$ that was adsorbed at 373 K on TiO_2 and then cooled to room temperature, $HCOOCH_3$ coadsorbed with H_2O, and $HCOOCH_3$ adsorbed at room temperature with vibrational modes in the alkyl (a) and carboxylate (b) regions.

4. Discussion

4.1. Methyl formate reaction pathway

The first step in the proposed reaction pathway is dissociation of MF to methoxy and formate [Reaction (1)]. Formate oxidizes directly to CO_2 [Reaction (2)], whereas methoxy reacts through formaldehyde and formate intermediates [16, 32,37–41] [Reaction (3)]. Note that O_2 consumption and H_2O production are not shown in the mechanism below for clarity.

$$H\,{}^{13}COOCH_3 \Rightarrow CH_3O_{(a)} + H\,{}^{13}COO_{(a)}, \quad (1)$$

$$H\,{}^{13}COO_{(a)} \Rightarrow {}^{13}CO_{2(g)}, \quad (2)$$

$$CH_3O_{(a)} \Rightarrow CH_2O_{(a)} \Rightarrow HCOO_{(a)} \Rightarrow CO_{2(g)}. \quad (3)$$

Methyl formate adsorbs on TiO_2 both molecularly and dissociatively as formate and methoxy (Fig. 1), in agreement with previous studies [18,37,42] of MF on various catalysts. Upon UV irradiation of a ^{13}MF monolayer, the $^{13}CO_2$ formation rate quickly reached a maximum (Fig. 2a). This indicates that the α-carbon in MF reacted directly to $^{13}CO_2$ without forming any long-lived intermediates [Reaction (2)], in agreement with previous studies of formic acid on TiO_2 [9,17]. However, the delayed maximum in the $^{12}CO_2$ formation rate (Fig. 2a) indicates that the β-carbon in MF oxidized to CO_2 through at least one intermediate. Using FTIR spectroscopy, Chuang et al. [15] reported that methoxy formed CO_2 through formaldehyde and formate intermediates during methanol PCO, in agreement with Busca [16].

Infrared spectra of methanol adsorbed on TiO_2 at room temperature (not shown) showed weak absorptions in the carboxylate region. Upon UV irradiation, however, strong bands characterizing a formate intermediate in the carboxylate (1640, 1575, 1380, and 1360 cm^{-1}) and alkyl (2865 and

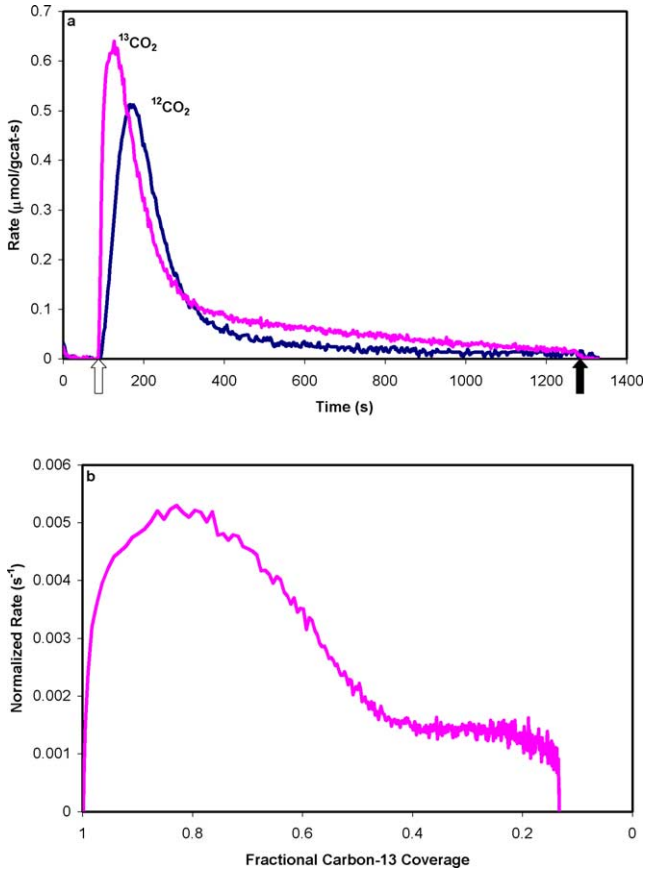

Fig. 7. Formation rates (a) and normalized $^{13}CO_2$ formation rate (b) during transient PCO of H $^{13}COOCH_3$ on TiO_2 carried out at 373 K. The UV lights were turned on (white arrow) at 60 s and turned off (black arrow) at 1260 s.

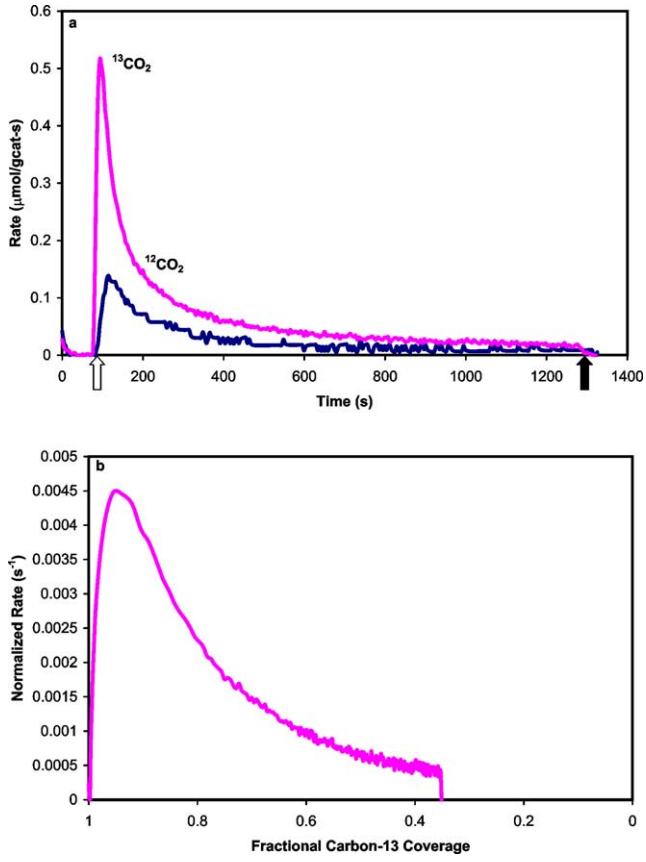

Fig. 8. Formation rates (a) and normalized $^{13}CO_2$ formation rate (b) during transient PCO of H $^{13}COOCH_3$ coadsorbed with H_2O at room temperature. The UV lights were turned on (white arrow) at 60 s and turned off (black arrow) at 1260 s.

2743 cm^{-1}) regions appeared immediately and decreased at longer reaction times. This indicates that PCO oxidized methoxy to formate, which formed CO_2 subsequently, as shown in Reaction (3). As noted previously, methoxy may oxidize to formate through a formaldehyde intermediate, but formaldehyde was not detected under the experimental conditions of this study. Similarly, DRIFTS spectra during ^{13}MF and D-MF PCO (not shown) showed that the intensity of absorption bands attributed to formate derived from the β-carbon in MF (2865, 2743, 1640, and 1380 cm^{-1}) initially *increased* and eventually decreased at longer reaction times. Although these initial increases cannot be seen during ^{12}MF PCO (Fig. 3a) because the UV intensity in Fig. 3 was greater than that during PCO of ^{13}MF and D-MF (not shown), Fig. 3b shows that absorptions at 2865, 2743, 1640, and 1380 cm^{-1} decreased slowly throughout PCO. That is, methoxy oxidized to CO_2 through intermediates [Reaction (3)] and produced the delayed $^{12}CO_2$ maximum in Fig. 2a.

4.2. Active sites

As discussed previously, the immediate maximum in the $^{13}CO_2$ formation rate (Fig. 2a) indicates that the α-carbon in MF oxidized directly to $^{13}CO_2$ in a single step. Therefore, the normalized $^{13}CO_2$ formation rate plotted versus fractional coverage measures directly the activity of TiO_2 adsorption sites. For a first-order, single-step reaction on a catalyst with one type of active site, a constant normalized rate would be expected because every site would oxidize adsorbed species at the same rate throughout transient PCO. Fig. 2b, however, shows clearly that the normalized $^{13}CO_2$ formation rate during ^{13}MF PCO varied considerably with coverage. At longer reaction times, the normalized $^{13}CO_2$ rate (Fig. 2b) approached a constant value that was approximately 20% of the initial maximum. This behavior is consistent with at least two types of active sites. Transient DRIFTS PCO (Fig. 3) also suggests multiple active sites for MF PCO on TiO_2. Upon UV irradiation of a MF monolayer, α-carbon formate absorptions at 1575, 1406, and 1367 cm^{-1} quickly decreased, yet that at 1556 cm^{-1} remained at longer reaction times (Fig. 3b).

The identification of two active sites explains the apparent discrepancy between transient and steady-state PCO observations. Formate oxidized quickly to $^{13}CO_2$ upon UV irradiation in Fig. 2a, yet Chuang et al. [18] reported that formate remained adsorbed on TiO_2 at longer irradiation times. The authors may have identified formate that was adsorbed on

less-active sites because these species are expected to remain on the surface after steady-state PCO. In contrast, the *initial* CO_2 formation rates in transient studies measure primarily the activity of sites that are more active during PCO. That is, MF reacts readily on more-active sites and yields high initial reaction rates during transient PCO.

4.3. Displacement of methyl formate by H_2O

If two sites of different activity existed, the normalized $^{13}CO_2$ rate would initially decrease, as species on more-active sites reacted, and eventually approach a constant value when species adsorbed primarily on less-active sites remained. However, the normalized $^{13}CO_2$ formation rate remained constant in Fig. 2b until approximately 30% of carbon-13 species reacted and subsequently decreased, approaching a constant value at low coverages. This initial, constant normalized rate was attributed to H_2O, a PCO product, displacing molecularly adsorbed MF, which readsorbs dissociatively on sites vacated during the initial stages of PCO. Because MF displacement by H_2O replenished active sites during PCO, the normalized $^{13}CO_2$ formation rate remained somewhat constant initially and subsequently decreased as PCO consumed the MF that was easily displaced.

Fig. 6 shows that preheating and coadsorbed H_2O displaced methoxy and molecularly adsorbed MF (2952, 2937, 2925, 2850, 2736, and 1310 cm^{-1}). As noted above, this displaced MF readsorbed dissociatively, which increased the coverage of α-carbon formate on more-active sites (1575 and 1367 cm^{-1}).

Preheating and coadsorbed H_2O also appear to displace the same weakly bound MF that is easily displaced by H_2O during room-temperature PCO because the normalized $^{13}CO_2$ formation rates during PCO with preheating (Fig. 4b) and with coadsorbed H_2O (Fig. 8b) began to decrease at higher coverages than that in Fig. 2b. That is, less molecularly bound MF was redistributed during subsequent PCO (Figs. 4b and 8b) because preheating and H_2O displaced weakly bound MF, which readsorbed dissociatively before PCO began. Additionally, adsorption at 373 K and coadsorbed H_2O removed methoxy and, therefore, less H_2O formed during PCO (three hydrogen atoms are bonded to the β-carbon, whereas the α-carbon only has one). That is, the normalized $^{13}CO_2$ formation rates (Figs. 4b and 8b) decreased at higher coverages than that in Fig. 2b partly because H_2O redistributed less MF to more-active sites during PCO. The effect of H_2O displacement during PCO is a significant finding that impacts the analysis of PCO rate data, particularly experiments that study PCO in the absence of gas-phase reactants.

4.4. Dual adsorption sites for methyl formate

Mass balances showed that preheating (Figs. 4 and 7) and coadsorbed H_2O (Fig. 8) removed methoxy from the surface, but did not change carbon-13 coverage. Because Fig. 6 shows that the coverage of molecularly adsorbed MF decreased, this displaced MF evidently readsorbed and dissociated on sites vacated by methoxy removal. Dissociative readsorption of this displaced MF apparently increased formate coverage on the *more-active* sites before PCO began because the maximum $^{13}CO_2$ formation rates during PCO with preheating (Fig. 4a) and with coadsorbed H_2O (Fig. 8a) were greater than that during room-temperature PCO (Fig. 2a).

If dual sites exist on TiO_2, in which several formate adsorption sites surround a single methoxy site, then removing methoxy may open dual sites for dissociation of displaced MF. That is, MF adsorption on dual sites appears to be limited by the availability of sites that adsorb methoxy. Using the same experimental apparatus as this study, Muggli and Backes [17] reported a formic acid monolayer coverage of 375 ± 25 μmol/g catalyst on TiO_2 that was 2.7 times that of MF (140 ± 10 μmol/g catalyst). In a similar study of methanol PCO on TiO_2, Schmidt [43] reported a methanol monolayer coverage on TiO_2 of 160 μmol/g catalyst. If the availability of methoxy sites constrains the number of dual sites for MF dissociation and formate sites are not saturated by a MF monolayer, then repeatedly removing methoxy and injecting MF would increase the formate coverage.

To explore the existence of dual sites, a series of experiments were performed, in which alternating 1-μL pulses of H_2O and ^{13}MF were injected after adsorbing a ^{13}MF monolayer at room temperature on TiO_2. Three $H_2O/^{13}MF$ injections *increased* carbon-13 coverage and decreased that of carbon-12 species by approximately 30 and 50%, respectively. Multiple $H_2O/^{13}MF$ injections apparently increased carbon-13 coverage by repeatedly opening dual sites for dissociative adsorption of MF through methoxy removal. Additionally, the intensity of α-carbon formate absorptions increased with each $H_2O/^{13}MF$ injection when this experiment was repeated with DRIFTS (not shown). This suggests that MF adsorbs dissociatively on dual sites composed of isolated methoxy sites surrounded by multiple formate sites. These dual sites will be studied in more detail in a forthcoming publication [36].

4.5. Heating increases intrinsic site activity

Elevated temperatures increased PCO rates on TiO_2. The initial normalized $^{13}CO_2$ formation rate during PCO at 373 K (Fig. 7b) was approximately 2.3 times that during room-temperature PCO (Fig. 2b). In a similar study of formic acid PCO on TiO_2, Muggli and Backes [17] reported that the initial normalized CO_2 formation rate at 373 K was also 2.3 times that at room temperature. The initial normalized $^{13}CO_2$ formation rate during PCO at 373 K (Fig. 7b) may be greater than that in Fig. 2b because elevated temperatures increased the mobility of surface species, which would replenish the more-active sites more quickly than at room temperature. Alternatively, heating may increase the activity of TiO_2 adsorption sites.

The normalized $^{13}CO_2$ formation rate during PCO at 373 K (Fig. 7b) began to decrease at a greater coverage (75% of a carbon-13 monolayer) than that during PCO of a monolayer (70% of a carbon-13 monolayer) (Fig. 2b). If elevated temperatures increased the mobility of surface species, then a greater fraction of adsorbed species would migrate to more-active sites vacated during PCO at 373 K than at room temperature. That is, the normalized $^{13}CO_2$ formation rate in Fig. 7b would be expected to decrease at a *lower* coverage than that during PCO of a monolayer (Fig. 2b). Because more-active sites oxidized a lesser fraction of surface species during PCO at 373 K (Fig. 7b) than during room-temperature PCO (Fig. 2b), elevated temperatures most likely do not increase the mobility of surface species. Instead, elevated temperatures increased the activity of both more- and less-active sites because the normalized $^{13}CO_2$ rate during PCO at 373 K was greater than that in Fig. 2b throughout PCO; the initial normalized rate measures primarily the activity of more-active sites, while less-active sites oxidize species predominantly at low coverages.

4.6. Heating and H_2O convert methoxy to formate

Fig. 6a shows that heating and coadsorbing H_2O removed methoxy (2952 and 2850 cm^{-1}) and converted some methoxy to formate (2743, 2865, and 1640 cm^{-1}). The conversion of methoxy to formate explains the interesting $^{12}CO_2$ formation curves in Fig. 5. Although carbon-12 coverages decreased upon heating or H_2O addition, Fig. 5 shows that methoxy initially oxidized to $^{12}CO_2$ more quickly than during room-temperature PCO. The $^{12}CO_2$ formation rate during room-temperature PCO (Fig. 5) would represent the maximum formation rate if MF and methoxy were the only carbon-12 surface species that participate in PCO because the catalyst surface was saturated at room temperature. That is, the $^{12}CO_2$ formation rates during PCO with preheating and coadsorbed H_2O would not exceed the room-temperature adsorption curve in Fig. 5. After 60 s of UV irradiation, however, the $^{12}CO_2$ formation rates during PCO with preheating and coadsorbed H_2O were approximately 1.3 times that during room-temperature PCO (Fig. 5). Additionally, the maximum $^{12}CO_2$ formation rates during PCO with coadsorbed H_2O and preheating occurred earlier in time than that during PCO of a monolayer (Fig. 5). This indicates that heating and H_2O addition converted the β-carbon in MF to a species (formate) that oxidized to $^{12}CO_2$ more quickly than methoxy.

4.7. Two-site model

The formation of gas-phase CO_2 monitors the surface reaction rate because it does not adsorb significantly on TiO_2 at room temperature and its appearance in the gas-phase is reaction limited [11,17,29]. The $^{13}CO_2$ formation rate measures directly the surface PCO rate of dissociated ^{13}MF because the α-carbon is expected to oxidize to CO_2 in a single step, in agreement with previous observations of other carboxylates [11,17,29]. As discussed previously, the immediate maximum in the $^{13}CO_2$ formation rate (Fig. 2a) indicates that the α-carbon reacted directly to $^{13}CO_2$ without forming any long-lived intermediates.

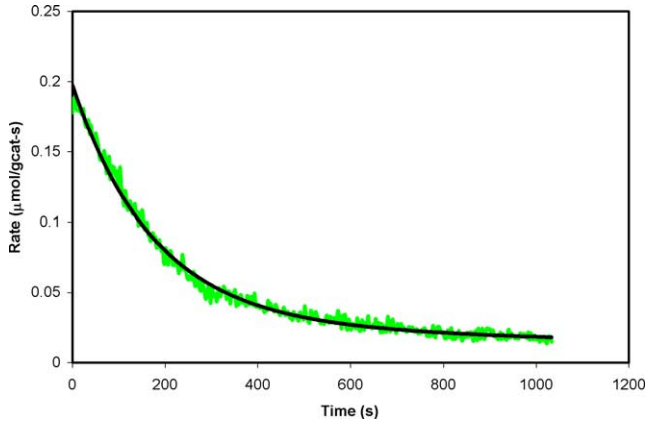

Fig. 9. Decay curve for $^{13}CO_2$ formation from H$^{13}COOCH_3$ PCO with two-site model fit.

During transient PCO of a ^{13}MF monolayer (Fig. 2b), the normalized $^{13}CO_2$ formation rate remained constant initially because H_2O, which is formed during PCO, displaced a fraction of weakly adsorbed MF. Subsequently, displaced MF readsorbed dissociatively as methoxy and formate on more-active sites vacated by PCO. After approximately 30% of carbon-13 species reacted, the normalized $^{13}CO_2$ formation rate began to decrease because nearly all of the MF that is easily displaced by H_2O was removed. A two-site model (Fig. 9) was fit to this portion of the $^{13}CO_2$ decay curve to quantify more- and less-active sites, along with their respective activities. The two-site model assumes constant oxygen concentration, and therefore first-order surface reactions.

Because mass balances determined the initial carbon-13 coverage, the model contained three adjustable parameters: site 1 activity (k_1), site 2 activity (k_2), and the ratio of site 1 and 2 coverages. The value determined for k_1 (6.0×10^{-3} s^{-1}) was approximately 13 times that of k_2 (4.8×10^{-4} s^{-1}), indicating a significant difference in activity. Approximately 30% of carbon-13 species adsorbed on the surface reacted on the more-active sites.

5. Conclusions

Methyl formate adsorbs on TiO_2 both molecularly and dissociatively on dual sites as formate and methoxy. The availability of methoxy sites limits dissociative adsorption of MF. During PCO on TiO_2, formate oxidizes to CO_2 in a single step without forming long-lived intermediates, whereas methoxy forms CO_2 through formaldehyde and formate. Water readily displaces molecularly adsorbed MF, which readsorbs dissociatively onto sites vacated during PCO. Approximately 30% of adsorption sites are highly active for

PCO; these sites are approximately 13 times more active than other adsorption sites. Heating and coadsorbing H_2O before MF PCO vacates dual sites for readsorption of molecularly adsorbed MF by removing methoxy from the surface. Preheating to 373 K and coadsorbing H_2O convert surface methoxy to formate. Elevated temperatures enhance the activity of TiO_2 adsorption sites, which increases PCO rates of both carbons in MF.

Acknowledgments

This material is based upon work supported by the National Science Foundation under Grants 0132289 and CTS 0223008. Acknowledgment is made to the Donors of the Petroleum Research Fund, administered by the American Chemical Society, and North Dakota Experimental Program to Stimulate Competitive Research (ND EPSCoR) for support of this research. A.C.L. gratefully acknowledges the Environmental Protection Agency Students Engaged in Environmental Research Program (EPA STEER) and the ND EPSCoR Advanced Undergraduate Research Award (AURA) Program.

References

[1] M.L. Sauer, D.F. Ollis, J. Catal. 149 (1994) 81.
[2] M.R. Nimlos, E.J. Wolfrum, M.L. Brewer, J.A. Fennell, G. Bintner, Environ. Sci. Technol. 30 (1996) 3102.
[3] A.V. Vorontsov, G.B. Barannik, O.I. Snegurenko, E.N. Savinov, V.N. Parmon, Kinet. Catal. 38 (1997) 84.
[4] N.R. Blake, G.L. Griffin, J. Phys. Chem. 92 (1988) 5697.
[5] J.C. Kennedy, A.K. Datye, J. Catal. 179 (1998) 375.
[6] J.L. Falconer, K.A. Magrini-Bair, J. Catal. 179 (1998) 171.
[7] D.S. Muggli, J.L. Falconer, J. Catal. 175 (1998) 213.
[8] D.S. Muggli, J.L. Falconer, J. Catal. 191 (2000) 318.
[9] D.S. Muggli, J.T. McCue, J.L. Falconer, J. Catal. 173 (1998) 470.
[10] D.S. Muggli, K.H. Lowery, J.L. Falconer, J. Catal. 180 (1998) 111.
[11] D.S. Muggli, S.A. Larson, J.L. Falconer, J. Phys. Chem. 100 (1996) 15886.
[12] W.A. Jacoby, D.M. Blake, R.D. Noble, C.A. Koval, J. Catal. 157 (1995) 87.
[13] G.Y. Popova, T.V. Andrushkevich, Y.A. Chesalov, E.S. Stoyanov, Kinet. Catal. 41 (2000) 805.
[14] L.F. Liao, W.C. Wu, C.Y. Chen, J.L. Lin, J. Phys. Chem. B 105 (2001) 7678.
[15] C.C. Chuang, C.C. Chen, J.L. Lin, J. Phys. Chem. B 103 (1999) 2439.
[16] G. Busca, J. Phys. Chem. 91 (1987) 5263.
[17] D.S. Muggli, M.J. Backes, J. Catal. 209 (2002) 105.
[18] C.C. Chuang, W.C. Wu, M.C. Huang, I.C. Huang, J.L. Lin, J. Catal. 185 (1999) 423.
[19] R. Zhang, Y. Sun, S. Peng, Fuel 81 (2002) 1619.
[20] E.A. a.G. Taylor, J. Phys. Chem. 92 (1988) 477.
[21] G.A.M. Hussein, N. Sheppard, M. Zaki, R.B. Fahim, J. Chem. Soc., Faraday Trans. 87 (1991) 2655.
[22] H. Onishi, T. Aruga, Y. Iwasawa, J. Catal. 146 (1994) 557.
[23] K.S. Kim, M.A. Barteau, Langmuir 4 (1988) 945.
[24] K.S. Kim, Langmuir 6 (1990) 1485.
[25] V.S. Lusvardi, M.A. Barteau, W.E. Farneth, J. Catal. 153 (1995) 41.
[26] S.A. Larson, J.A. Widegren, J.L. Falconer, J. Catal. 157 (1995) 611.
[27] D.S. Muggli, L.F. Ding, Appl. Catal. B Environ. 32 (2001) 181.
[28] D.S. Muggli, L.F. Ding, M.J. Odland, Catal. Lett. 78 (2002) 23.
[29] D.S. Muggli, J.L. Falconer, J. Catal. 187 (1999) 230.
[30] D.S. Muggli, J.L. Falconer, J. Catal. 181 (1999) 155.
[31] D.S. Muggli, S.A. Keyser, J.L. Falconer, Catal. Lett. 55 (1998) 129.
[32] D.S. Muggli, M.J. Odland, L.R. Schmidt, J. Catal. 203 (2001) 51.
[33] G.Y. Popova, Y.A. Chesalove, T.V. Andrushkevich, E.S. Stoyanov, React. Kinet. Catal. Lett. 76 (2002) 123.
[34] L.B. Lambert, H.F. Shurvell, D.A. Lightner, R.G. Cooks, Organic Structural Spectroscopy, Prentice Hall, NJ, 1998.
[35] W.C. Wu, C.C. Chuang, J.L. Lin, J. Phys. Chem. B 104 (2000) 8719.
[36] S. Mischke, A.C. Lukaski, D.S. Muggli, in preparation.
[37] M. Bowker, H. Houghton, K.C. Waugh, J. Chem. Soc., Faraday Trans., 1 78 (1982) 2573.
[38] V. Lochar, J. Machek, J. Tichy, Appl. Catal. A 228 (2002) 95.
[39] G.J. Millar, C.H. Rochester, K.C. Waugh, J. Catal. 142 (1993) 263.
[40] X.D. Peng, Surf. Sci. 224 (1989) 327.
[41] S.L. Silva, A.A. Patel, T.M. Pham, F.M. Leibsle, Surf. Sci. 441 (1999) 351.
[42] J.M. Vohs, M.A. Barteau, Surf. Sci. 197 (1988) 109.
[43] L.R. Schmidt, Trichloroethylene Mixture Effects During Transient Photocatalytic Oxidation of Methanol, Univ. of North Dakota, 2000.